BABAR-PUB-06/047
SLAC-PUB-12030

Improved Measurements of the Branching Fractions for $B^0 \to \pi^+\pi^-$ and $B^0 \to K^+\pi^-$, and a Search for $B^0 \to K^+K^-$

B. Aubert,[1] R. Barate,[1] M. Bona,[1] D. Boutigny,[1] F. Couderc,[1] Y. Karyotakis,[1] J. P. Lees,[1] V. Poireau,[1] V. Tisserand,[1] A. Zghiche,[1] E. Grauges,[2] A. Palano,[3] J. C. Chen,[4] N. D. Qi,[4] G. Rong,[4] P. Wang,[4] Y. S. Zhu,[4] G. Eigen,[5] I. Ofte,[5] B. Stugu,[5] G. S. Abrams,[6] M. Battaglia,[6] D. N. Brown,[6] J. Button-Shafer,[6] R. N. Cahn,[6] E. Charles,[6] M. S. Gill,[6] Y. Groysman,[6] R. G. Jacobsen,[6] J. A. Kadyk,[6] L. T. Kerth,[6] Yu. G. Kolomensky,[6] G. Kukartsev,[6] G. Lynch,[6] L. M. Mir,[6] T. J. Orimoto,[6] M. Pripstein,[6] N. A. Roe,[6] M. T. Ronan,[6] W. A. Wenzel,[6] P. del Amo Sanchez,[7] M. Barrett,[7] K. E. Ford,[7] T. J. Harrison,[7] A. J. Hart,[7] C. M. Hawkes,[7] S. E. Morgan,[7] A. T. Watson,[7] T. Held,[8] H. Koch,[8] B. Lewandowski,[8] M. Pelizaeus,[8] K. Peters,[8] T. Schroeder,[8] M. Steinke,[8] J. T. Boyd,[9] J. P. Burke,[9] W. N. Cottingham,[9] D. Walker,[9] T. Cuhadar-Donszelmann,[10] B. G. Fulsom,[10] C. Hearty,[10] N. S. Knecht,[10] T. S. Mattison,[10] J. A. McKenna,[10] A. Khan,[11] P. Kyberd,[11] M. Saleem,[11] D. J. Sherwood,[11] L. Teodorescu,[11] V. E. Blinov,[12] A. D. Bukin,[12] V. P. Druzhinin,[12] V. B. Golubev,[12] A. P. Onuchin,[12] S. I. Serednyakov,[12] Yu. I. Skovpen,[12] E. P. Solodov,[12] K. Yu Todyshev,[12] D. S. Best,[13] M. Bondioli,[13] M. Bruinsma,[13] M. Chao,[13] S. Curry,[13] I. Eschrich,[13] D. Kirkby,[13] A. J. Lankford,[13] P. Lund,[13] M. Mandelkern,[13] R. K. Mommsen,[13] W. Roethel,[13] D. P. Stoker,[13] S. Abachi,[14] C. Buchanan,[14] S. D. Foulkes,[15] J. W. Gary,[15] O. Long,[15] B. C. Shen,[15] K. Wang,[15] L. Zhang,[15] H. K. Hadavand,[16] E. J. Hill,[16] H. P. Paar,[16] S. Rahatlou,[16] V. Sharma,[16] J. W. Berryhill,[17] C. Campagnari,[17] A. Cunha,[17] B. Dahmes,[17] T. M. Hong,[17] D. Kovalskyi,[17] J. D. Richman,[17] T. W. Beck,[18] A. M. Eisner,[18] C. J. Flacco,[18] C. A. Heusch,[18] J. Kroseberg,[18] W. S. Lockman,[18] G. Nesom,[18] T. Schalk,[18] B. A. Schumm,[18] A. Seiden,[18] P. Spradlin,[18] D. C. Williams,[18] M. G. Wilson,[18] J. Albert,[19] E. Chen,[19] A. Dvoretskii,[19] F. Fang,[19] D. G. Hitlin,[19] I. Narsky,[19] T. Piatenko,[19] F. C. Porter,[19] A. Ryd,[19] A. Samuel,[19] G. Mancinelli,[20] B. T. Meadows,[20] K. Mishra,[20] M. D. Sokoloff,[20] F. Blanc,[21] P. C. Bloom,[21] S. Chen,[21] W. T. Ford,[21] J. F. Hirschauer,[21] A. Kreisel,[21] M. Nagel,[21] U. Nauenberg,[21] A. Olivas,[21] W. O. Ruddick,[21] J. G. Smith,[21] K. A. Ulmer,[21] S. R. Wagner,[21] J. Zhang,[21] A. Chen,[22] E. A. Eckhart,[22] A. Soffer,[22] W. H. Toki,[22] R. J. Wilson,[22] F. Winklmeier,[22] Q. Zeng,[22] D. D. Altenburg,[23] E. Feltresi,[23] A. Hauke,[23] H. Jasper,[23] A. Petzold,[23] B. Spaan,[23] T. Brandt,[24] V. Klose,[24] H. M. Lacker,[24] W. F. Mader,[24] R. Nogowski,[24] J. Schubert,[24] K. R. Schubert,[24] R. Schwierz,[24] J. E. Sundermann,[24] A. Volk,[24] D. Bernard,[25] G. R. Bonneaud,[25] P. Grenier,[25,*] E. Latour,[25] Ch. Thiebaux,[25] M. Verderi,[25] P. J. Clark,[26] W. Gradl,[26] F. Muheim,[26] S. Playfer,[26] A. I. Robertson,[26] Y. Xie,[26] M. Andreotti,[27] D. Bettoni,[27] C. Bozzi,[27] R. Calabrese,[27] G. Cibinetto,[27] E. Luppi,[27] M. Negrini,[27] A. Petrella,[27] L. Piemontese,[27] E. Prencipe,[27] F. Anulli,[28] R. Baldini-Ferroli,[28] A. Calcaterra,[28] R. de Sangro,[28] G. Finocchiaro,[28] S. Pacetti,[28] P. Patteri,[28] I. M. Peruzzi,[28,†] M. Piccolo,[28] M. Rama,[28] A. Zallo,[28] A. Buzzo,[29] R. Capra,[29] R. Contri,[29] M. Lo Vetere,[29] M. M. Macri,[29] M. R. Monge,[29] S. Passaggio,[29] C. Patrignani,[29] E. Robutti,[29] A. Santroni,[29] S. Tosi,[29] G. Brandenburg,[30] K. S. Chaisanguanthum,[30] M. Morii,[30] J. Wu,[30] R. S. Dubitzky,[31] J. Marks,[31] S. Schenk,[31] U. Uwer,[31] D. J. Bard,[32] W. Bhimji,[32] D. A. Bowerman,[32] P. D. Dauncey,[32] U. Egede,[32] R. L. Flack,[32] J. A. Nash,[32] M. B. Nikolich,[32] W. Panduro Vazquez,[32] P. K. Behera,[33] X. Chai,[33] M. J. Charles,[33] U. Mallik,[33] N. T. Meyer,[33] V. Ziegler,[33] J. Cochran,[34] H. B. Crawley,[34] L. Dong,[34] V. Eyges,[34] W. T. Meyer,[34] S. Prell,[34] E. I. Rosenberg,[34] A. E. Rubin,[34] A. V. Gritsan,[35] A. G. Denig,[36] M. Fritsch,[36] G. Schott,[36] N. Arnaud,[37] M. Davier,[37] G. Grosdidier,[37] A. Höcker,[37] F. Le Diberder,[37] V. Lepeltier,[37] A. M. Lutz,[37] A. Oyanguren,[37] S. Pruvot,[37] S. Rodier,[37] P. Roudeau,[37] M. H. Schune,[37] A. Stocchi,[37] W. F. Wang,[37] G. Wormser,[37] C. H. Cheng,[38] D. J. Lange,[38] D. M. Wright,[38] C. A. Chavez,[39] I. J. Forster,[39] J. R. Fry,[39] E. Gabathuler,[39] R. Gamet,[39] K. A. George,[39] D. E. Hutchcroft,[39] D. J. Payne,[39] K. C. Schofield,[39] C. Touramanis,[39] A. J. Bevan,[40] F. Di Lodovico,[40] W. Menges,[40] R. Sacco,[40] G. Cowan,[41] H. U. Flaecher,[41] D. A. Hopkins,[41] P. S. Jackson,[41] T. R. McMahon,[41] S. Ricciardi,[41] F. Salvatore,[41] A. C. Wren,[41] D. N. Brown,[42] C. L. Davis,[42] J. Allison,[43] N. R. Barlow,[43] R. J. Barlow,[43] Y. M. Chia,[43] C. L. Edgar,[43] G. D. Lafferty,[43] M. T. Naisbit,[43] J. C. Williams,[43] J. I. Yi,[43] C. Chen,[44] W. D. Hulsbergen,[44] A. Jawahery,[44] C. K. Lae,[44] D. A. Roberts,[44] G. Simi,[44] G. Blaylock,[45] C. Dallapiccola,[45] S. S. Hertzbach,[45] X. Li,[45] T. B. Moore,[45] S. Saremi,[45] H. Staengle,[45] R. Cowan,[46] G. Sciolla,[46] S. J. Sekula,[46] M. Spitznagel,[46] F. Taylor,[46] R. K. Yamamoto,[46] H. Kim,[47] S. E. Mclachlin,[47] P. M. Patel,[47] S. H. Robertson,[47] A. Lazzaro,[48] V. Lombardo,[48] F. Palombo,[48] J. M. Bauer,[49] L. Cremaldi,[49] V. Eschenburg,[49] R. Godang,[49] R. Kroeger,[49] D. A. Sanders,[49] D. J. Summers,[49] H. W. Zhao,[49] S. Brunet,[50] D. Côté,[50] M. Simard,[50] P. Taras,[50] F. B. Viaud,[50] H. Nicholson,[51] N. Cavallo,[52,‡] G. De Nardo,[52]

F. Fabozzi,[52,‡] C. Gatto,[52] L. Lista,[52] D. Monorchio,[52] P. Paolucci,[52] D. Piccolo,[52] C. Sciacca,[52] M. Baak,[53] G. Raven,[53] H. L. Snoek,[53] C. P. Jessop,[54] J. M. LoSecco,[54] T. Allmendinger,[55] G. Benelli,[55] K. K. Gan,[55] K. Honscheid,[55] D. Hufnagel,[55] P. D. Jackson,[55] H. Kagan,[55] R. Kass,[55] A. M. Rahimi,[55] R. Ter-Antonyan,[55] Q. K. Wong,[55] N. L. Blount,[56] J. Brau,[56] R. Frey,[56] O. Igonkina,[56] M. Lu,[56] R. Rahmat,[56] N. B. Sinev,[56] D. Strom,[56] J. Strube,[56] E. Torrence,[56] A. Gaz,[57] M. Margoni,[57] M. Morandin,[57] A. Pompili,[57] M. Posocco,[57] M. Rotondo,[57] F. Simonetto,[57] R. Stroili,[57] C. Voci,[57] M. Benayoun,[58] J. Chauveau,[58] H. Briand,[58] P. David,[58] L. Del Buono,[58] Ch. de la Vaissière,[58] O. Hamon,[58] B. L. Hartfiel,[58] M. J. J. John,[58] Ph. Leruste,[58] J. Malclès,[58] J. Ocariz,[58] L. Roos,[58] G. Therin,[58] L. Gladney,[59] J. Panetta,[59] M. Biasini,[60] R. Covarelli,[60] C. Angelini,[61] G. Batignani,[61] S. Bettarini,[61] F. Bucci,[61] G. Calderini,[61] M. Carpinelli,[61] R. Cenci,[61] F. Forti,[61] M. A. Giorgi,[61] A. Lusiani,[61] G. Marchiori,[61] M. A. Mazur,[61] M. Morganti,[61] N. Neri,[61] E. Paoloni,[61] G. Rizzo,[61] J. J. Walsh,[61] M. Haire,[62] D. Judd,[62] D. E. Wagoner,[62] J. Biesiada,[63] N. Danielson,[63] P. Elmer,[63] Y. P. Lau,[63] C. Lu,[63] J. Olsen,[63] A. J. S. Smith,[63] A. V. Telnov,[63] E. Baracchini,[64] F. Bellini,[64] G. Cavoto,[64] A. D'Orazio,[64] D. del Re,[64] E. Di Marco,[64] R. Faccini,[64] F. Ferrarotto,[64] F. Ferroni,[64] M. Gaspero,[64] L. Li Gioi,[64] M. A. Mazzoni,[64] S. Morganti,[64] G. Piredda,[64] F. Polci,[64] F. Safai Tehrani,[64] C. Voena,[64] M. Ebert,[65] H. Schröder,[65] R. Waldi,[65] T. Adye,[66] N. De Groot,[66] B. Franek,[66] E. O. Olaiya,[66] F. F. Wilson,[66] R. Aleksan,[67] S. Emery,[67] A. Gaidot,[67] S. F. Ganzhur,[67] G. Hamel de Monchenault,[67] W. Kozanecki,[67] M. Legendre,[67] G. Vasseur,[67] Ch. Yèche,[67] M. Zito,[67] X. R. Chen,[68] H. Liu,[68] W. Park,[68] M. V. Purohit,[68] J. R. Wilson,[68] M. T. Allen,[69] D. Aston,[69] R. Bartoldus,[69] P. Bechtle,[69] N. Berger,[69] R. Claus,[69] J. P. Coleman,[69] M. R. Convery,[69] M. Cristinziani,[69] J. C. Dingfelder,[69] J. Dorfan,[69] G. P. Dubois-Felsmann,[69] D. Dujmic,[69] W. Dunwoodie,[69] R. C. Field,[69] T. Glanzman,[69] S. J. Gowdy,[69] M. T. Graham,[69] V. Halyo,[69] C. Hast,[69] T. Hryn'ova,[69] W. R. Innes,[69] M. H. Kelsey,[69] P. Kim,[69] D. W. G. S. Leith,[69] S. Li,[69] S. Luitz,[69] V. Luth,[69] H. L. Lynch,[69] D. B. MacFarlane,[69] H. Marsiske,[69] R. Messner,[69] D. R. Muller,[69] C. P. O'Grady,[69] V. E. Ozcan,[69] A. Perazzo,[69] M. Perl,[69] T. Pulliam,[69] B. N. Ratcliff,[69] A. Roodman,[69] A. A. Salnikov,[69] R. H. Schindler,[69] J. Schwiening,[69] A. Snyder,[69] J. Stelzer,[69] D. Su,[69] M. K. Sullivan,[69] K. Suzuki,[69] S. K. Swain,[69] J. M. Thompson,[69] J. Va'vra,[69] N. van Bakel,[69] M. Weaver,[69] A. J. R. Weinstein,[69] W. J. Wisniewski,[69] M. Wittgen,[69] D. H. Wright,[69] A. K. Yarritu,[69] K. Yi,[69] C. C. Young,[69] P. R. Burchat,[70] A. J. Edwards,[70] S. A. Majewski,[70] B. A. Petersen,[70] C. Roat,[70] L. Wilden,[70] S. Ahmed,[71] M. S. Alam,[71] R. Bula,[71] J. A. Ernst,[71] V. Jain,[71] B. Pan,[71] M. A. Saeed,[71] F. R. Wappler,[71] S. B. Zain,[71] W. Bugg,[72] M. Krishnamurthy,[72] S. M. Spanier,[72] R. Eckmann,[73] J. L. Ritchie,[73] A. Satpathy,[73] C. J. Schilling,[73] R. F. Schwitters,[73] J. M. Izen,[74] X. C. Lou,[74] S. Ye,[74] F. Bianchi,[75] F. Gallo,[75] D. Gamba,[75] M. Bomben,[76] L. Bosisio,[76] C. Cartaro,[76] F. Cossutti,[76] G. Della Ricca,[76] S. Dittongo,[76] L. Lanceri,[76] L. Vitale,[76] V. Azzolini,[77] F. Martinez-Vidal,[77] Sw. Banerjee,[78] B. Bhuyan,[78] C. M. Brown,[78] D. Fortin,[78] K. Hamano,[78] R. Kowalewski,[78] I. M. Nugent,[78] J. M. Roney,[78] R. J. Sobie,[78] J. J. Back,[79] P. F. Harrison,[79] T. E. Latham,[79] G. B. Mohanty,[79] M. Pappagallo,[79] H. R. Band,[80] X. Chen,[80] B. Cheng,[80] S. Dasu,[80] M. Datta,[80] K. T. Flood,[80] J. J. Hollar,[80] P. E. Kutter,[80] B. Mellado,[80] A. Mihalyi,[80] Y. Pan,[80] M. Pierini,[80] R. Prepost,[80] S. L. Wu,[80] Z. Yu,[80] and H. Neal[81]

(The *BABAR* Collaboration)

[1]*Laboratoire de Physique des Particules, F-74941 Annecy-le-Vieux, France*
[2]*Universitat de Barcelona, Facultat de Fisica Dept. ECM, E-08028 Barcelona, Spain*
[3]*Università di Bari, Dipartimento di Fisica and INFN, I-70126 Bari, Italy*
[4]*Institute of High Energy Physics, Beijing 100039, China*
[5]*University of Bergen, Institute of Physics, N-5007 Bergen, Norway*
[6]*Lawrence Berkeley National Laboratory and University of California, Berkeley, California 94720, USA*
[7]*University of Birmingham, Birmingham, B15 2TT, United Kingdom*
[8]*Ruhr Universität Bochum, Institut für Experimentalphysik 1, D-44780 Bochum, Germany*
[9]*University of Bristol, Bristol BS8 1TL, United Kingdom*
[10]*University of British Columbia, Vancouver, British Columbia, Canada V6T 1Z1*
[11]*Brunel University, Uxbridge, Middlesex UB8 3PH, United Kingdom*
[12]*Budker Institute of Nuclear Physics, Novosibirsk 630090, Russia*
[13]*University of California at Irvine, Irvine, California 92697, USA*
[14]*University of California at Los Angeles, Los Angeles, California 90024, USA*
[15]*University of California at Riverside, Riverside, California 92521, USA*
[16]*University of California at San Diego, La Jolla, California 92093, USA*
[17]*University of California at Santa Barbara, Santa Barbara, California 93106, USA*
[18]*University of California at Santa Cruz, Institute for Particle Physics, Santa Cruz, California 95064, USA*
[19]*California Institute of Technology, Pasadena, California 91125, USA*
[20]*University of Cincinnati, Cincinnati, Ohio 45221, USA*
[21]*University of Colorado, Boulder, Colorado 80309, USA*
[22]*Colorado State University, Fort Collins, Colorado 80523, USA*

[23] Universität Dortmund, Institut für Physik, D-44221 Dortmund, Germany
[24] Technische Universität Dresden, Institut für Kern- und Teilchenphysik, D-01062 Dresden, Germany
[25] Ecole Polytechnique, Laboratoire Leprince-Ringuet, F-91128 Palaiseau, France
[26] University of Edinburgh, Edinburgh EH9 3JZ, United Kingdom
[27] Università di Ferrara, Dipartimento di Fisica and INFN, I-44100 Ferrara, Italy
[28] Laboratori Nazionali di Frascati dell'INFN, I-00044 Frascati, Italy
[29] Università di Genova, Dipartimento di Fisica and INFN, I-16146 Genova, Italy
[30] Harvard University, Cambridge, Massachusetts 02138, USA
[31] Universität Heidelberg, Physikalisches Institut, Philosophenweg 12, D-69120 Heidelberg, Germany
[32] Imperial College London, London, SW7 2AZ, United Kingdom
[33] University of Iowa, Iowa City, Iowa 52242, USA
[34] Iowa State University, Ames, Iowa 50011-3160, USA
[35] Johns Hopkins University, Baltimore, Maryland 21218, USA
[36] Universität Karlsruhe, Institut für Experimentelle Kernphysik, D-76021 Karlsruhe, Germany
[37] Laboratoire de l'Accélérateur Linéaire, IN2P3-CNRS et Université Paris-Sud 11, Centre Scientifique d'Orsay, B.P. 34, F-91898 ORSAY Cedex, France
[38] Lawrence Livermore National Laboratory, Livermore, California 94550, USA
[39] University of Liverpool, Liverpool L69 7ZE, United Kingdom
[40] Queen Mary, University of London, E1 4NS, United Kingdom
[41] University of London, Royal Holloway and Bedford New College, Egham, Surrey TW20 0EX, United Kingdom
[42] University of Louisville, Louisville, Kentucky 40292, USA
[43] University of Manchester, Manchester M13 9PL, United Kingdom
[44] University of Maryland, College Park, Maryland 20742, USA
[45] University of Massachusetts, Amherst, Massachusetts 01003, USA
[46] Massachusetts Institute of Technology, Laboratory for Nuclear Science, Cambridge, Massachusetts 02139, USA
[47] McGill University, Montréal, Québec, Canada H3A 2T8
[48] Università di Milano, Dipartimento di Fisica and INFN, I-20133 Milano, Italy
[49] University of Mississippi, University, Mississippi 38677, USA
[50] Université de Montréal, Physique des Particules, Montréal, Québec, Canada H3C 3J7
[51] Mount Holyoke College, South Hadley, Massachusetts 01075, USA
[52] Università di Napoli Federico II, Dipartimento di Scienze Fisiche and INFN, I-80126, Napoli, Italy
[53] NIKHEF, National Institute for Nuclear Physics and High Energy Physics, NL-1009 DB Amsterdam, The Netherlands
[54] University of Notre Dame, Notre Dame, Indiana 46556, USA
[55] Ohio State University, Columbus, Ohio 43210, USA
[56] University of Oregon, Eugene, Oregon 97403, USA
[57] Università di Padova, Dipartimento di Fisica and INFN, I-35131 Padova, Italy
[58] Universités Paris VI et VII, Laboratoire de Physique Nucléaire et de Hautes Energies, F-75252 Paris, France
[59] University of Pennsylvania, Philadelphia, Pennsylvania 19104, USA
[60] Università di Perugia, Dipartimento di Fisica and INFN, I-06100 Perugia, Italy
[61] Università di Pisa, Dipartimento di Fisica, Scuola Normale Superiore and INFN, I-56127 Pisa, Italy
[62] Prairie View A&M University, Prairie View, Texas 77446, USA
[63] Princeton University, Princeton, New Jersey 08544, USA
[64] Università di Roma La Sapienza, Dipartimento di Fisica and INFN, I-00185 Roma, Italy
[65] Universität Rostock, D-18051 Rostock, Germany
[66] Rutherford Appleton Laboratory, Chilton, Didcot, Oxon, OX11 0QX, United Kingdom
[67] DSM/Dapnia, CEA/Saclay, F-91191 Gif-sur-Yvette, France
[68] University of South Carolina, Columbia, South Carolina 29208, USA
[69] Stanford Linear Accelerator Center, Stanford, California 94309, USA
[70] Stanford University, Stanford, California 94305-4060, USA
[71] State University of New York, Albany, New York 12222, USA
[72] University of Tennessee, Knoxville, Tennessee 37996, USA
[73] University of Texas at Austin, Austin, Texas 78712, USA
[74] University of Texas at Dallas, Richardson, Texas 75083, USA
[75] Università di Torino, Dipartimento di Fisica Sperimentale and INFN, I-10125 Torino, Italy
[76] Università di Trieste, Dipartimento di Fisica and INFN, I-34127 Trieste, Italy
[77] IFIC, Universitat de Valencia-CSIC, E-46071 Valencia, Spain
[78] University of Victoria, Victoria, British Columbia, Canada V8W 3P6
[79] Department of Physics, University of Warwick, Coventry CV4 7AL, United Kingdom
[80] University of Wisconsin, Madison, Wisconsin 53706, USA
[81] Yale University, New Haven, Connecticut 06511, USA

(Dated: August 2, 2006)

We present measurements of the branching fractions for the charmless two-body decays $B^0 \to \pi^+\pi^-$ and $B^0 \to K^+\pi^-$, and a search for the decay $B^0 \to K^+K^-$. We include the effects of final-state radiation from the daughter mesons for the first time, and quote branching fractions for the inclusive processes $B^0 \to h^+h'^-n\gamma$, where h and h' are pions or kaons. The maximum value of the sum of the energies of the n undetected photons, $E_\gamma^{\rm max}$, is mode-dependent. Using a data sample of approximately 227 million $\Upsilon(4S) \to B\overline{B}$ decays collected with the *BABAR* detector at the PEP-II asymmetric-energy e^+e^- collider at SLAC, we measure:

$$\begin{aligned}
\mathcal{B}(B^0 \to \pi^+\pi^- n\gamma;\ E_\gamma^{\rm max} = 150\,{\rm MeV}) &= (5.4 \pm 0.4 \pm 0.3) \times 10^{-6},\\
\mathcal{B}(B^0 \to K^+\pi^- n\gamma;\ E_\gamma^{\rm max} = 105\,{\rm MeV}) &= (18.6 \pm 0.6 \pm 0.6) \times 10^{-6},\\
\mathcal{B}(B^0 \to K^+K^- n\gamma;\ E_\gamma^{\rm max} = 59\,{\rm MeV}) &< 0.40 \times 10^{-6}\,(90\%\ \text{confidence level}),
\end{aligned}$$

where the first uncertainty is statistical and the second is systematic. Theoretical calculations can be used to extrapolate from the above measurements the non-radiative branching fractions, $\mathcal{B}^0$. Using one such calculation, we find:

$$\begin{aligned}
\mathcal{B}^0(B^0 \to \pi^+\pi^-) &= (5.8 \pm 0.4 \pm 0.3) \times 10^{-6},\\
\mathcal{B}^0(B^0 \to K^+\pi^-) &= (19.7 \pm 0.6 \pm 0.6) \times 10^{-6},\\
\mathcal{B}^0(B^0 \to K^+K^-) &< 0.40 \times 10^{-6}\,(90\%\ \text{confidence level}).
\end{aligned}$$

Meaningful comparison between theory and experiment, as well as combination of measurements from different experiments, can be performed only in terms of these non-radiative quantities.

PACS numbers: 13.25.Hw, 12.15.Hh, 11.30.Er

Charmless hadronic two-body B decays to pions and kaons provide a wealth of information on *CP* violation in the B system, including all angles of the unitarity triangle. The time-dependent *CP* asymmetries in the $\pi\pi$ system can be used to estimate the angle α [1]; the decay rates for the $K\pi$ channels provide information on γ [2]. Recently, direct *CP* violation in decay was established in the B system through observation of a significant rate asymmetry between $B^0 \to K^+\pi^-$ and $\overline{B}^0 \to K^-\pi^+$ decays [3, 4]. As B physics experiments accumulate much larger data sets, charmless two-body B decays will continue to play a fundamental role in testing the standard model description of *CP* violation. Measurements of branching fractions for all the charmless two-body decays are invaluable in testing the various theoretical approaches to the underlying hadron dynamics citethy. We present measurements of branching fractions for the decays $B^0 \to \pi^+\pi^-$ and $K^+\pi^-$ [6], and a search for the decay $B^0 \to K^+K^-$ using a data sample about 2.5 times larger than that used for the most precise, previously published measurements [7, 8] of these quantities.

As radiative corrections have already proved to be important in precise determinations of interesting quantities in the context of kaon physics [9], we account for them in this analysis as well. We can relate the observable decay rates $\Gamma_{hh'}(E_\gamma^{\rm max})$ for $B^0 \to h^+h'^-n\gamma$ (and thus the branching fractions) to the theoretical non-radiative widths $\Gamma^0_{hh'}$, using the energy-dependent correction factors $G_{hh'}(E_\gamma^{\rm max};\mu)$ [10]

$$\begin{aligned}
\Gamma_{hh'}(E_\gamma^{\rm max}) &= \Gamma(B^0 \to h^+h^-n\gamma)|_{\sum E_\gamma < E_\gamma^{\rm max}}\\
&= \Gamma^0_{hh'}(\mu)\, G_{hh'}(E_\gamma^{\rm max};\mu), \qquad (1)
\end{aligned}$$

where $E_\gamma^{\rm max}$ is the maximum value allowed for the sum of the undetected photon energies and μ is the renormalization scale at which $\Gamma^0_{hh'}$ and $G_{hh'}(E_\gamma^{\rm max})$ are calculated (the product being independent of μ). Extracting $\Gamma^0_{hh'}$ allows a more meaningful comparison with theoretical calculations and also between different experimental results. Additionally, for $E_\gamma^{\rm max}$ at the kinematic limit, G approaches unity (to order $\alpha_{\rm QED}/\pi$), so that the $\Gamma^0_{hh'}$, and the corresponding branching fractions, can be interpreted theoretically in a cleaner way.

The data sample used for this analysis contains $(226.6 \pm 2.5) \times 10^6$ $\Upsilon(4S) \to B\overline{B}$ decays collected by the *BABAR* detector [11] at the SLAC PEP-II e^+e^- asymmetric-energy storage ring. The primary detector components used in the analysis are a charged-particle tracking system consisting of a five-layer silicon vertex detector and a 40-layer drift chamber surrounded by a 1.5-T solenoidal magnet, an electromagnetic calorimeter comprising 6580 CsI(Tl) crystals, and a dedicated particle-identification system consisting of a detector of internally reflected Cherenkov light providing at least 3 σ K–π separation over the range of laboratory momentum relevant for this study (1.5–4.5 GeV/c).

The data sample used in this analysis is similar to that used in the *BABAR* measurements of direct *CP* violation in $B^0 \to K^+\pi^-$ [3] and time-dependent *CP*-violating asymmetry amplitudes $S_{\pi\pi}$ and $C_{\pi\pi}$ in $B^0 \to \pi^+\pi^-$ [12] (the reader is referred to those references for further de-

*Also at Laboratoire de Physique Corpusculaire, Clermont-Ferrand, France
†Also with Università di Perugia, Dipartimento di Fisica, Perugia, Italy
‡Also with Università della Basilicata, Potenza, Italy

tails of the analysis technique). Event selection criteria are identical to those used in the *CP* analyses [3, 12], except that we remove the requirement on the difference in the decay times (Δt) between the two B mesons in order to minimize systematic uncertainties on the branching fraction measurements.

We identify $B^0 \to h^+h'^-$ ($h, h' = \pi$ or K) candidates with selection requirements on track and Cherenkov angle (θ_c) quality, B decay kinematic variables, and event topology.

The final sample contains 69264 events and is defined by requirements on two kinematic variables: (1) the difference $\Delta E = E_B^* - \sqrt{s}/2$ between the reconstructed energy of the B candidate in the e^+e^- center-of-mass (CM) frame and $\sqrt{s}/2$; and (2) the beam-energy substituted mass $m_{\rm ES} = \sqrt{(s/2 + \mathbf{p}_i \cdot \mathbf{p_B})^2/E_i^2 - \mathbf{p_B}^2}$. Here, $\sqrt{s}$ is the total CM energy, and the B momentum $\mathbf{p_B}$ and the four-momentum $(E_i, \mathbf{p_i})$ of the e^+e^- initial state are defined in the laboratory frame. To simplify the analysis, we use the pion mass for all tracks in the track reconstruction and the calculation of the kinematic variables. We select those B candidates with $|\Delta E| < 150\,\mathrm{MeV}$, and $5.20 < m_{\rm ES} < 5.29\,\mathrm{GeV}/c^2$.

The efficiencies of the selection criteria are determined in samples of GEANT-4 based [13] Monte Carlo (MC) simulated signal decays, where we include the effects of electromagnetic radiation from the final-state charged particles using the PHOTOS simulation package [14]. We compare the performance of our simulation with a scalar QED calculation up to $\mathcal{O}(\alpha_{\rm QED})$ [10] and reweight the ΔE distributions for each mode to account for the general underestimation of the number of radiating events found in our simulation. For the final maximum likelihood fit, we then fix the parameters describing the radiative tail of ΔE to the values determined from the reweighted distributions.

As explained in Ref. [10], while taking into account radiative corrections, one needs to be careful to quote the results in such a way that the radiation effects can be disentangled. In principle, it would be necessary to select B candidates with a specified maximum amount of $\mathcal{O}(100\,\mathrm{MeV})$ photon energy in the final state, a quantity that is difficult to reconstruct with the *BABAR* detector. Instead, we define our data sample by selecting on ΔE, an observable that can be clearly related to the maximum allowed total energy of the photons, $E_\gamma^{\rm max}$. The chosen ΔE window allows for the presence of radiated photons with total energy up to $150\,\mathrm{MeV} + \langle \Delta E \rangle$, where the average value of ΔE, $\langle \Delta E \rangle$, differs for each mode, due to the pion mass hypothesis being assigned to all tracks. As the $\pi^+\pi^-$ events are centered at $\Delta E \sim 0\,\mathrm{MeV}$, while the $K^+\pi^-$ and K^+K^- distributions are shifted by $-45\,\mathrm{MeV}$ and $-91\,\mathrm{MeV}$, respectively, the corresponding energy requirements on the radiated photons are $E_\gamma^{\rm max} = 150$, 105 and 59 MeV for $\pi^+\pi^-$, $K^+\pi^-$, and K^+K^-, respectively. The smearing of ΔE due to finite momentum resolution leads to a small difference between the number of events that satisfy the ΔE requirement and the number of events that satisfy an equivalent $E_\gamma^{\rm max}$ requirement. We thus correct the efficiencies for this effect ($1.0-2.6\%$, depending on the channel).

TABLE I: Summary of total detection efficiencies (%) for signal decays determined in Monte Carlo simulated samples without final-state radiation effects (No FSR), compared with the results using PHOTOS and the leading-order scalar QED calculation. Uncertainties are statistical only.

Mode	No FSR	PHOTOS	QED $\mathcal{O}(\alpha_{\rm QED})$
$\pi^+\pi^-$	41.6 ± 0.2	41.0 ± 0.2	40.3 ± 0.2
$K^+\pi^-$	40.5 ± 0.2	39.9 ± 0.2	39.3 ± 0.2
K^+K^-	38.7 ± 0.3	38.7 ± 0.3	38.5 ± 0.3

For comparison purposes, we summarize in Table I the efficiencies for the different modes for three separate cases, as determined from the MC simulation: assuming no final-state radiation (FSR); using PHOTOS to simulate FSR; and, in addition to PHOTOS, applying corrections to the efficiencies from the QED calculation, as described above. For the nominal branching fraction measurement we use the efficiency as determined using the simulation corrected with the QED calculation, and take the difference with respect to the uncorrected PHOTOS simulation as a systematic uncertainty.

In addition to signal $\pi^+\pi^-$, $K^+\pi^-$, and (possibly) K^+K^- events, the selected data sample includes background from the process $e^+e^- \to q\bar{q}$ ($q = u, d, s, c$). According to the MC simulation, backgrounds from other B decays are small relative to the signal yields ($< 1\%$), and are treated as a systematic uncertainty. We use an unbinned, extended maximum-likelihood (ML) fit to extract simultaneously signal and background yields in the three topologies ($\pi\pi$, $K\pi$, and KK). The fit uses the discriminating variables $m_{\rm ES}$, ΔE, the Cherenkov angles of the two tracks, and a Fisher discriminant $\mathcal{F}$, based on the momentum flow relative to the $h^+h'^-$ thrust axis of all tracks and clusters in the event, excluding the $h^+h'^-$ pair, as described in Ref. [7]. The likelihood for event j is obtained by summing the product of the event yield N_i and probability $\mathcal{P}_i$ over the signal and background hypotheses i. The total likelihood for a sample of N events is

$$\mathcal{L} = \frac{1}{N!} \exp\left(-\sum_i N_i\right) \prod_j \left[\sum_i N_i \mathcal{P}_i(\vec{x}_j; \vec{\alpha}_i)\right]. \quad (2)$$

The probabilities $\mathcal{P}_i$ are evaluated as the product of the probability density functions (PDFs) with parameters $\vec{\alpha}_i$, for each of the independent variables $\vec{x}_j = \{m_{\rm ES}, \Delta E, \mathcal{F}, \theta_c^+, \theta_c^-\}$, where θ_c^+ and θ_c^- are the Cherenkov angles for the positively- and negatively-charged tracks, respectively. We check that the variables are almost independent. The largest correlation between the $\vec{x}_j$ is 13% for the pair $(m_{\rm ES}, \Delta E)$, and we have confirmed that it has a negligible effect on the fitted yields.

For both signal and background, the $K^{\pm}\pi^{\mp}$ yields are parameterized as $N_{K^{\pm}\pi^{\mp}} = N_{K\pi}\left(1 \mp \mathcal{A}_{K\pi}\right)/2$, and we fit directly for the total yield $N_{K\pi}$ and the asymmetry $\mathcal{A}_{K\pi}$. The result for $\mathcal{A}_{K\pi}$ is used only as a consistency check and does not supersede our previously published result [3].

The eight parameters describing the background shapes for $m_{\rm ES}$, ΔE, and $\mathcal{F}$ are allowed to vary freely in the ML fit. We use a threshold function [15] for $m_{\rm ES}$ (one parameter), a second-order polynomial for ΔE (two parameters), and a sum of two Gaussian distributions for $\mathcal{F}$ (five parameters). For the signal shape in $m_{\rm ES}$, we use a single Gaussian distribution to describe all three channels and allow the mean and width to vary in the fit. For ΔE, we use the sum of two Gaussian distributions (core + tail), where the core parameters are common to all channels and are allowed to vary freely, and the tail parameters are determined separately for each channel from the reweighted MC simulation (explained above), and fixed in the fit. For the signal shape in $\mathcal{F}$, we use an asymmetric Gaussian function with different widths below and above the mean. All three parameters are determined from MC simulation and fixed in the maximum-likelihood fit. The θ_c PDFs are obtained from a sample of approximately 430000 $D^{*+} \to D^0\pi^+ (D^0 \to K^-\pi^+)$ decays reconstructed in data, where K^-/π^+ tracks are identified through the charge correlation with the π^+ from the D^{*+} decay. We construct the PDFs separately for K^+, K^-, π^+, and π^- tracks as a function of momentum and polar angle using the measured and expected values of θ_c, and its uncertainty. We use the same PDFs for tracks in signal and background events.

Table II summarizes the fitted signal and background yields, and $K\pi$ charge asymmetries. We find a value of $\mathcal{A}_{K\pi}$ consistent with our previously published result [3], and a background asymmetry consistent with zero. The signal yields are slightly higher than the values reported in Ref. [3] due to the removal of the Δt selection requirement and the addition of the radiative tail in the signal ΔE PDF. In order to quantify the effect of FSR on the fitted yields, we perform a second fit using a single Gaussian for the ΔE PDF, allowing the mean and width to vary. The results are shown in the second column of Table II, where we find that ignoring FSR lowers the $\pi\pi$ yield by 4.3% and the $K\pi$ yield by 1.6%.

As a crosscheck, in Fig. 1 we compare the PDF shapes (solid curves) to the data using the event-weighting technique described in Ref. [16]. For each plot, we perform a fit excluding the variable being plotted and use the fitted yields and covariance matrix to determine the relative probability that an event is signal or background. The distribution is normalized to the yield for the given component and can be compared directly to the assumed PDF shape. We find excellent agreement between the data and the PDFs. Figure 2 shows the likelihood ratio $\mathcal{L}_S/\sum\mathcal{L}_i$ for all 69264 events in the fitted sample, where $\mathcal{L}_S$ is the likelihood for a given signal hypothesis, and the summation in the denominator is over all signal and background components in the fit. We find good agreement between data (points with error bars) and the distributions obtained by directly generating events from the PDFs (histograms).

TABLE II: Summary of results from the ML fit for the yields. The subscript b refers to background. For the nominal fit, we use a double Gaussian for the signal ΔE PDF, as described in the text. We also show, for comparison purposes, the results using a single Gaussian, which corresponds to an analysis that ignores FSR effects.

Parameter	Nominal Fit	Ignoring FSR
$N_{\pi\pi}$	489 ± 35	469 ± 34
$N_{K\pi}$	1660 ± 52	1634 ± 52
$\mathcal{A}_{K\pi}$	-0.136 ± 0.030	-0.135 ± 0.030
N_{KK}	3 ± 13	5 ± 13
$N_{b\pi\pi}$	32979 ± 194	32998 ± 194
$N_{bK\pi}$	20775 ± 169	20801 ± 169
$\mathcal{A}_{bK\pi}$	0.002 ± 0.008	0.002 ± 0.008
N_{bKK}	13358 ± 126	13356 ± 126

TABLE III: Summary of relative systematic uncertainties on yields, efficiencies, and number of $B\overline{B}$ pairs. For the K^+K^- yield we show the absolute uncertainty. The total uncertainties are calculated as the sum in quadrature of the individual contributions.

Source	$\pi^+\pi^-$	$K^+\pi^-$	K^+K^-
yields	3.8%	1.8%	6.8 events
efficiency	3.0%	2.5%	2.0%
$N_{B\overline{B}}$	1.1%	1.1%	1.1%
Total	5.0%	3.3%	see text

Systematic uncertainties on the branching fractions arise from uncertainties on the selection efficiency, signal yield, and number of $B\overline{B}$ events in the sample. Uncertainty on the efficiency is dominated by track reconstruction (1.6%) and the effect of FSR (2.0%), which is taken to be the difference in efficiency before and after applying the QED correction to the simulation (Table I). Uncertainty on the fitted signal yields is dominated by the shape of the signal PDF for $\mathcal{F}$ (2.9% for $\pi\pi$, 1.5% for $K\pi$) and potential bias (2.2% for $\pi\pi$, 0.9% for $K\pi$) in the fitting technique, as determined from large samples of MC-simulated signal events and a large ensemble of pseudo-experiments generated from the PDF shapes. Uncertainties due to imperfect knowledge of the PDF shapes for $m_{\rm ES}$, ΔE, and θ_c are all less than 1%. Table III summarizes the total uncertainty on each of the branching fractions, which is calculated as the sum in quadrature of the individual uncertainties.

Table IV summarizes the results for the charge-averaged branching fractions. For comparison, we use the efficiencies and signal yields determined under the assumption of no FSR and find $\mathcal{B}(B^0 \to \pi^+\pi^-) = 5.1 \times 10^{-6}$ and $\mathcal{B}(B^0 \to K^+\pi^-) = 18.1 \times 10^{-6}$, which

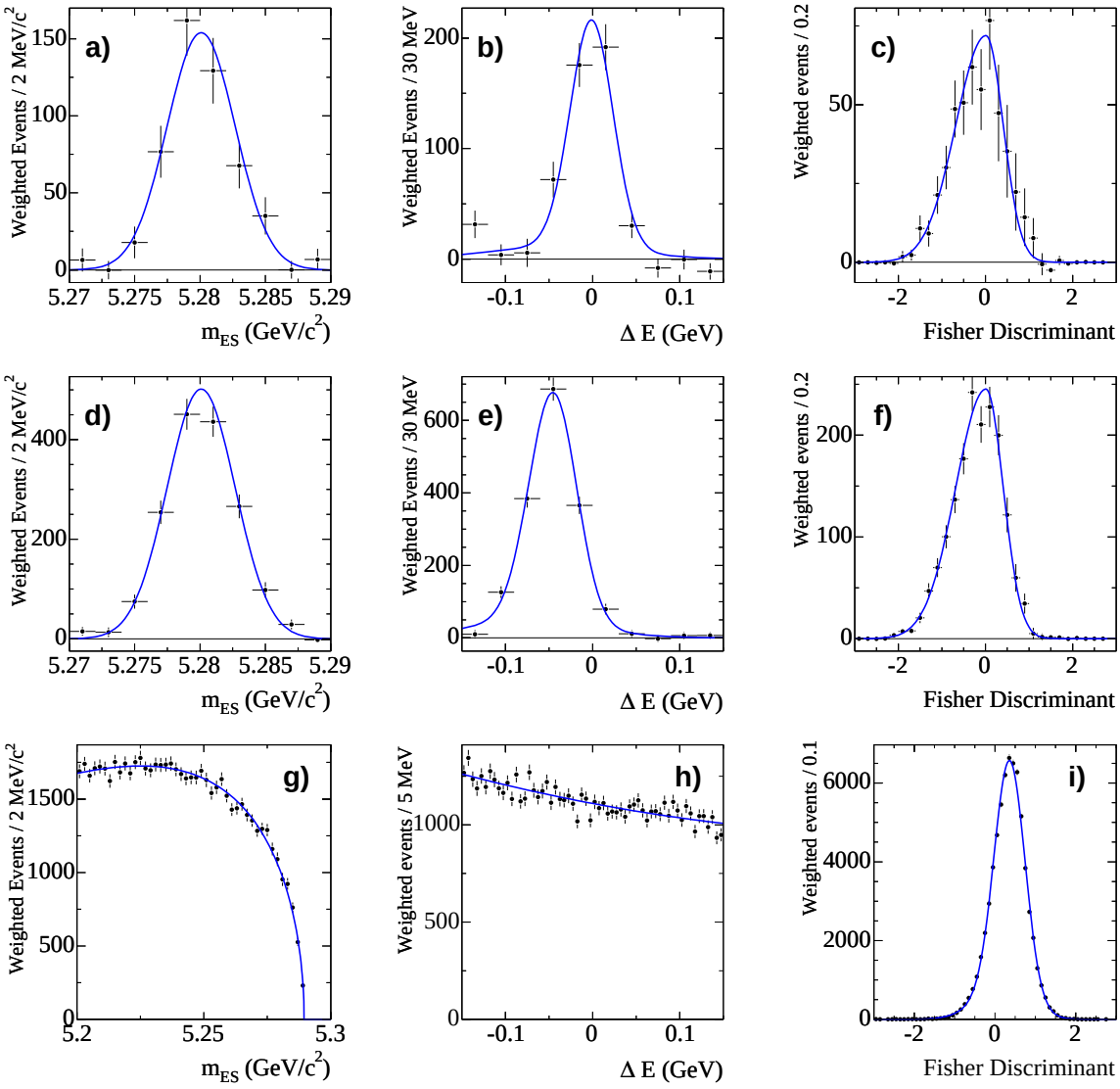

FIG. 1: Data distributions (points with error bars) of $m_{\rm ES}$, ΔE, and $\mathcal{F}$ for signal $\pi^+\pi^-$ (a,b,c), signal $K^+\pi^-$ (d,e,f) and background for the three channels (g,h,i), using the weighting technique described in the text. Solid curves represent the corresponding PDFs used in the fit. The distribution of ΔE for signal $K^+\pi^-$ events is shifted due to the assignment of the pion mass for all tracks.

are consistent with our previously published results [7]. Taking into account FSR effects leads to an increase of the branching fractions by approximately 6% and 3% for $\pi^+\pi^-$ and $K^+\pi^-$, respectively. We determine the upper limit for the signal yield for K^+K^- using a Bayesian procedure that assumes a flat prior on the number of events. The upper limit is given by the value of N_0 for which $\int_0^{N_0} \mathcal{L}_{\rm max}\, dN / \int_0^{\infty} \mathcal{L}_{\rm max}\, dN = 0.90$, corresponding to a one-sided 90% confidence interval. Here, $\mathcal{L}_{\rm max}$ is the likelihood as a function of the K^+K^- yield N, maximized with respect to the remaining fit parameters. We find $N_0 = 26.2$, and the upper limit on the branching fraction is calculated by increasing the signal yield upper limit and reducing the efficiency by their respective total errors (Table III). For the purpose of combining with measurements by other experiments, we also evaluate the central value for the branching fraction and find $\mathcal{B}(B^0 \to K^+K^-n\gamma) = (4 \pm 15 \pm 8) \times 10^{-8}$.

Although we cannot directly measure the non-radiative, or "bare" branching fractions, due to the intrinsic and unavoidable features of QED, they can be extrapolated from our measurements by employing theoretical calculations, such as those found in Ref. [10]. The results for these bare branching fractions for the three channels are shown in Table V, and the central value for the bare K^+K^- branching fraction is $\mathcal{B}(B^0 \to K^+K^-) = (5 \pm 15 \pm 8) \times 10^{-8}$. We stress the importance of being able to disentangle radiation effects from the ex-

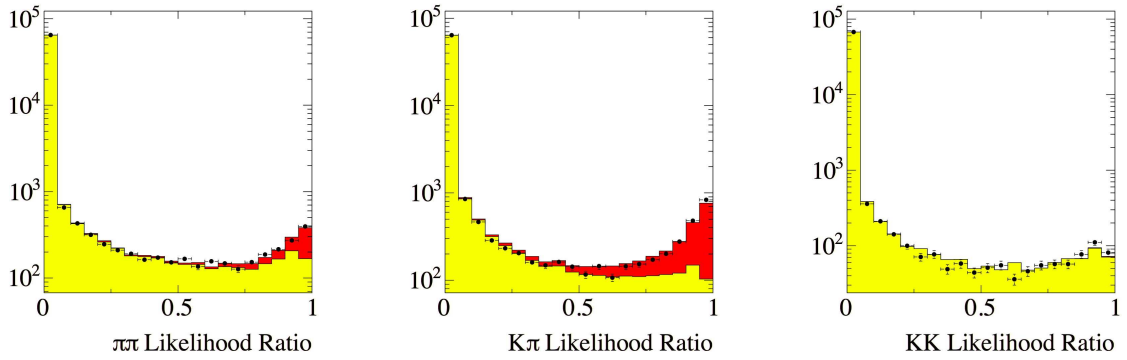

FIG. 2: (Color online) Distribution of the likelihood ratio $\mathcal{L}_S/\sum\mathcal{L}_i$, where $\mathcal{L}_S$ is the likelihood for each event to be a signal $\pi^+\pi^-$ (left), $K^+\pi^-$ (middle), or K^+K^- (right) event. The points with error bars show the distribution obtained on the fitted data sample, while the histograms show the distributions obtained by generating signal (dark shaded, red) and background (light shaded, yellow) events directly from the PDFs.

TABLE IV: Summary of branching fraction results. We give signal yields N_S, total detection efficiencies (ϵ) and branching fractions $\mathcal{B}_{E_\gamma}$, where the subscript E_γ serves as a reminder of the dependence on the cut on soft photon energy as explained in the text. The errors are statistical and systematic, respectively, and the upper limit on $B^0 \to K^+K^-n\gamma$ corresponds to the 90% confidence level.

Mode	N_S	$\epsilon\,(\%)$	$\mathcal{B}_{E_\gamma}(10^{-6})$
$\pi^+\pi^-$	$489 \pm 35 \pm 11$	$40.3 \pm 0.2 \pm 1.2$	$5.4 \pm 0.4 \pm 0.3$
$K^+\pi^-$	$1660 \pm 52 \pm 15$	$39.3 \pm 0.2 \pm 1.0$	$18.6 \pm 0.6 \pm 0.6$
K^+K^-	$3.3 \pm 13.1 \pm 6.8$	$38.5 \pm 0.3 \pm 0.8$	< 0.40 (90% C.L.)

TABLE V: Summary of experimental branching fractions, $\mathcal{B}_{E_\gamma}$, with a defined cut on soft photon energy, together with the electromagnetic correction factor $G(E_\gamma^{\rm max})$ and the evaluated "bare" branching fractions (non radiative), $\mathcal{B}^0$. The errors on branching fractions are statistical and systematic respectively; the error on $G(E_\gamma^{\rm max})$ is taken as the difference between its value at $\mu = M_\pi$ and $\mu = M_\rho$.

Mode	$\mathcal{B}_{E_\gamma}(10^{-6})$	$G(E_\gamma^{\rm max})$	$\mathcal{B}^0(10^{-6})$
$\pi^+\pi^-$	$5.4 \pm 0.4 \pm 0.3$	0.935 ± 0.005	$5.8 \pm 0.4 \pm 0.3$
$K^+\pi^-$	$18.6 \pm 0.6 \pm 0.6$	0.944 ± 0.005	$19.7 \pm 0.6 \pm 0.6$
K^+K^-	< 0.40 (90% C.L.)	0.952 ± 0.005	< 0.40 (90% C.L.)

perimental measurements, as a meaningful comparison between theory and experiment can be performed only in terms of the bare quantities. Likewise, bare quantities should be used when combining measurements from different experiments.

In summary, we have presented updated measurements of charge-averaged branching fractions for the decays $B^0 \to \pi^+\pi^-$ and $B^0 \to K^+\pi^-$, with FSR effects taken into account. We find that the branching fractions are 3-6% higher when the effect of FSR is included in the calculation of the efficiency and signal yield determination. This difference should be taken into account when comparing with previous measurements of these quantities [7, 8, 17] that do not include these effects. In order to perform the most meaningful comparison, we also evaluated the bare branching fractions for the three channels, as explained in Ref. [10]. Our results are consistent with current theoretical estimates from different models [5]. We find no evidence for the decay $B^0 \to K^+K^-$ and set an upper limit of 4.0×10^{-7} at the 90% confidence level.

We are grateful for the excellent luminosity and machine conditions provided by our PEP-II colleagues, and for the substantial dedicated effort from the computing organizations that support *BABAR*. The collaborating institutions wish to thank SLAC for its support and kind hospitality. This work is supported by DOE and NSF (USA), NSERC (Canada), IHEP (China), CEA and CNRS-IN2P3 (France), BMBF and DFG (Germany), INFN (Italy), FOM (The Netherlands), NFR (Norway), MIST (Russia), MEC (Spain), and PPARC (United Kingdom). Individuals have received support from the Marie Curie EIF (European Union) and the A. P. Sloan Foundation.

[1] M. Gronau, Phys. Rev. Lett. **63**, 1451 (1989); M. Gronau and D. London, Phys. Rev. Lett. **65**, 3381 (1990).
[2] M. Gronau, J. L. Rosner, and D. London, Phys. Rev. Lett. **73**, 21 (1994); R. Fleischer and T. Mannel, Phys. Rev. D **57**, 2752 (1998); M. Neubert and J. L. Rosner, Phys. Lett. B **441**, 403 (1998); A. J. Buras and R. Fleis-

cher, Eur. Phys. Jour. C **11**, 93 (1999); for a recent review see M. Gronau and J. L. Rosner, SLAC-R-709, hep-ph 0503261.
[3] *BABAR* Collaboration, B. Aubert *et al.*, Phys. Rev. Lett. **93**, 131801 (2004).
[4] Belle Collaboration, Y. Chao *et al.*, Phys. Rev. Lett. **93**, 191802 (2004).
[5] M. Ciuchini *et al.*, Phys. Lett. B **515**, 33 (2001); C. W. Bauer, S. Fleming, D. Pirjol, and I. W. Stewart, Phys. Rev. D **63**, 114020 (2001); M. Beneke and M. Neubert, Nucl. Phys. B **675**, 333 (2003); J. Charles *et al.*, Eur. Phys. Jour. C **31**, 503 (2003); Y.-Y. Keum, Pramana **63**, 1151 (2004); C.-W. Chiang, M. Gronau, J. L. Rosner, and D. A. Suprun, Phys. Rev. D **70**, 034020 (2004); A. J. Buras, R. Fleischer, S. Recksiegel, and F. Schwab, Nucl. Phys. B **697**, 133 (2004).
[6] The use of charge conjugate modes is implied throughout this paper unless otherwise stated.
[7] *BABAR* Collaboration, B. Aubert *et al.*, Phys. Rev. Lett. **89**, 281802 (2002).
[8] Belle Collaboration, Y. Chao *et al.*, Phys. Rev. D **69**, 111102 (2004).
[9] KLOE Collaboration, F. Ambrosino *et al.*, Phys. Lett. B **632**, 43 (2006).
[10] E. Baracchini and G. Isidori, Phys. Lett. B **633**, 309 (2006).
[11] *BABAR* Collaboration, B. Aubert *et al.*, Nucl. Instrum. Methods **A479**, 1 (2002).
[12] *BABAR* Collaboration, B. Aubert *et al.*, Phys. Rev. Lett. **95**, 151803 (2005).
[13] S. Agostinelli *et al.* Nucl. Instrum. Methods **A506**, 250 (2003).
[14] E. Barberio and Z. Was, Comput. Phys. Commun. **79**, 291 (1994). We use version 2.03.
[15] ARGUS Collaboration, H. Albrecht *et al.*, Z. Phys. C **48**, 543 (1990).
[16] M. Pivk and F. R. Le Diberder, Nucl. Instrum. Methods **A555**, 356 (2005).
[17] CLEO Collaboration, A. Bornheim *et al.*, Phys. Rev. D **68**, 052002 (2003).

Abstract

We present measurements of the branching fractions for the charmless two-body decays $B^0 \to \pi^+\pi^-$ and $B^0 \to K^+\pi^-$, and a search for the decay $B^0 \to K^+K^-$. We include the effects of final-state radiation from the daughter mesons for the first time, and quote branching fractions for the inclusive processes $B^0 \to h^+h'^-n\gamma$, where h and h' are pions or kaons. The maximum value of the sum of the energies of the n undetected photons, $E_\gamma^{\rm max}$, is mode-dependent. Using a data sample of approximately 227 million $\Upsilon(4S) \to B\bar{B}$ decays collected with the BaBar detector at the PEP-II asymmetric-energy e^+e^- collider at SLAC, we measure:

$$\begin{aligned}
\mathcal{B}(B^0 \to \pi^+\pi^-, n\gamma;\ E_\gamma^{\rm max} = 150MeV) &= (5.4 \pm 0.4 \pm 0.3) \times 10^{-6}, \\
\mathcal{B}(B^0 \to K^+\pi^-, n\gamma;\ E_\gamma^{\rm max} = 105MeV) &= (18.6 \pm 0.6 \pm 0.6) \times 10^{-6}, \\
\mathcal{B}(B^0 \to K^+K^-, n\gamma;\ E_\gamma^{\rm max} = 59MeV) &< 0.40 \times 10^{-6}\,(90\%\ \text{confidence level}),
\end{aligned}$$

where the first uncertainty is statistical and the second is systematic. Theoretical calculations can be used to extrapolate from the above measurements the non-radiative branching fractions, $\mathcal{B}^0$. Using one such calculation, we find:

$$\begin{aligned}
\mathcal{B}^0(B^0 \to \pi^+\pi^-) &= (5.8 \pm 0.4 \pm 0.3) \times 10^{-6}, \\
\mathcal{B}^0(B^0 \to K^+\pi^-) &= (19.7 \pm 0.6 \pm 0.6) \times 10^{-6}, \\
\mathcal{B}^0(B^0 \to K^+K^-) &< 0.40 \times 10^{-6}\,(90\%\ \text{confidence level}).
\end{aligned}$$

Meaningful comparison between theory and experiment, as well as combination of measurements from different experiments, can be performed only in terms of these non-radiative quantities.